Total and Sand Floodplain Deposition on an Inside Bend During the 2019 Missouri River Flood

Michael Mansfield, P.E.[1] (Michael.P.Mansfield@usace.army.mil),
John Shelley, Ph.D., P.E.[1] (John.Shelley@usace.army.mil), and Stanford Gibson, Ph.D.[2]
[1]*River Engineering and Restoration Section, U.S. Army Corps of Engineers, Kansas City, Missouri, United States*
[2]*Hydrologic Engineering Center, Institute for Water Resources, U.S. Army Corps of Engineers, Davis, California, United States*

ABSTRACT

Elwood Bottoms is a wildlife reserve that lies on the west side of the Missouri River, across from St. Joseph, Missouri. In 2019, the Missouri River inundated Elwood Bottoms for 73 days, much longer than the 1.85-day annual average outside of major flood events. This paper analyzes the floodplain deposition on Elwood Bottoms during the 2019 flood using repeated LiDAR, ground-based cross section surveys, and sediment sample datasets. The 2019 flood deposited 215,000 m^3 of sediment on this floodplain. Sand concentrations in the deposits ranged from 8% to 100%. The authors computed a spatially varying sand fraction and used it to estimate a total sand deposition of 93,000 m^3, roughly one-third the sediment volume scoured in the channel along the same reach during the flood. The computed sand deposit exceeded previous estimates for a similar long-term flood in 2011 by a factor of 3.5, which might stem from better computational methods or might reflect actual differences in the depositional behavior of the events. Floodplain deposits generally thinned and fined with distance from the channel, and subsurface samples were coarser than surface samples. The surficial 90th percentile of grain size distribution (d_{90}) decreased by an order of magnitude across the deposits, from approximately 0.1 mm close to the channel to 0.01 mm at the distal edge of the inundated floodplain.

INTRODUCTION

Floodplain deposition is a major sediment sink during flood events on sand-bed rivers (Aalto et al., 2003; Gibson and Shelley, 2020; He and Walling, 1996; Kiss et al., 2011). For example, Gibson and Shelley (2020) estimated that the amount of overbank sand deposition during a 2011 flood on the lower 500 miles of the Missouri River roughly corresponded with the total volume of bed change within the channel. Jacobson and Oberg (1997) reported that the floodplain deposition on the Mississippi River during a 1993 flood event was approximately 22–36% of the total sediment load. Ten Brinke et al. (1998) estimated that the overbank sand deposition during 1993–1995 floods on the Rhine River in the Netherlands approximately equaled the amount of sand entering the reach. Such large sediment sinks provide context for river response post-flood and must be accounted for in sediment budgets. In rivers that have not undergone substantial stabilization efforts for navigation, this sediment sink would eventually be reintroduced into the river as the river meandered throughout the floodplain. However, for rivers that have been stabilized for navigation (such as the Missouri and Mississippi rivers), this sediment is essentially removed from the system forever, as floods are nearly always net depositional in the floodplain. Past attempts to quantify floodplain deposition have relied upon aerial photography and field investigations, rather than using Light Detection and Ranging (LiDAR) technology (Alexander et al.,

Midcontinent Geoscience • Volume 5 • August 2024

Midcontinent Geoscience is an open-access, peer-reviewed journal of the Kansas Geological Survey. The journal publishes original research on a broad array of geoscience topics, with an emphasis on the midcontinent region of the United States, including the Great Plains and Central Lowland provinces.

2013; He and Walling, 1996; Ten Brinke et al., 1998). The present analysis contributes significantly to the field of geomorphology by using new LiDAR technology to accurately calculate elevation changes in the floodplain as the result of a major flood in 2019. Sediment samples collected in the floodplain allowed for a computation of the sand fraction of the overbank deposits.

With regard to the relationship between sediment gradation and distance from the bank, fining with distance from the bank is a well-documented phenomenon (Branß et al., 2016; Lecce and Pavlowsky, 2004; Pizzuto, 1987). Several models have been developed to understand this relationship, including Pizzuto (1987) and James (1985). Both of these models relied on turbulent diffusion to determine the fining trend with distance from the bank. Pizzuto (1987) concluded that the diffusion model could accurately characterize the morphology of the floodplain but that it could not accurately predict the grain size distribution. He theorized that this was due to advection and bedload transport, which potentially dominated the deposition pattern. The research presented in this paper addressed independent yet related questions: (1) How does the total volume of sand deposited by the Missouri River on Elwood Bottoms during the 2019 flood compare to the total volume of scour in the adjacent reach? (2) How does the size of the deposited sediment vary with distance from the bank?

STUDY AREA

Elwood Bottoms is a wildlife area located along the right descending bank of the Missouri River near St. Joseph, Missouri (fig. 1). The area encompasses approximately 1,116 acres (451 hectares). The main vegetation present at this site is eastern cottonwood trees (KDWP, 2022). The U.S. Army Corps of Engineers (USACE) purchased the land between 2006 and 2015 under Water Resources Development Acts authorizations. Elwood Bottoms is now managed by USACE and the Kansas Department of Wildlife and Parks (KDWP, 2022). Elwood Bottoms is frequently inundated by the Missouri River and excess runoff.

Since 1990, three major floods have inundated Elwood Bottoms for extended periods (table 1). Outside of these three events, the Missouri River inundates Elwood Bottoms an average of 1.85 days per year.

The 1993, 2011, and 2019 floods inundated Elwood Bottoms for a total of 194 days. In the remaining 27 years since 1990, Elwood Bottoms was inundated for a combined 50 days. Between the 2011 and the 2019 flood events, Elwood Bottoms was inundated for a total of four days (see fig. 2 for St. Joseph water surface elevation plot). Major floods deliver a greater proportion of the total floodplain sediment than the time of inundation would suggest because the sediment loads at St. Joseph grow exponentially with flow (USACE,

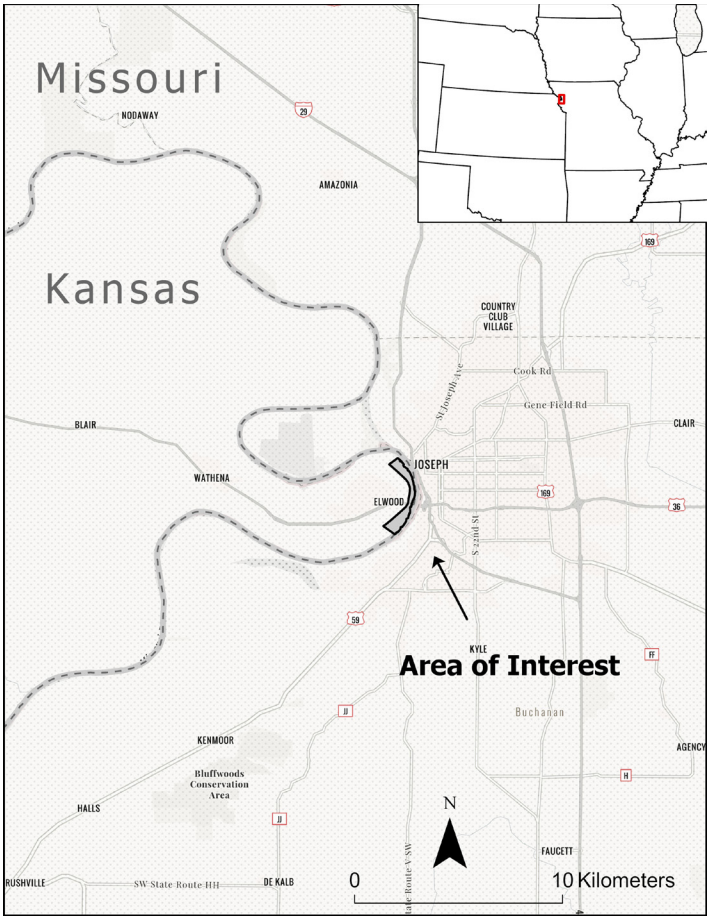

Figure 1. Elwood Bottoms boundary and vicinity.

Table 1. Elwood Bottoms inundation history since 1990.

Year	Annual Flood Frequency (yr)[1]	Days Inundated/Year
1993	80	30
2011	35	91
2019	63	73
Average of all other years in period of record (1990–2020)	-	1.85
Average annual inundation days, 2012–2018	-	0.67

[1]Based on logarithmic interpolation of regulated flow values reported in the 2023 Missouri River Flow Frequency Study (USACE, 2023).

2017; Abraham et al., 2017). Therefore, the vast majority of floodplain-available sediment is deposited during these large events. This paper will analyze the total deposition in the Elwood Bottoms area as a result of the 2019 flood, the amount of sand deposition from the 2019 flood, the volume of scour in the adjacent river reach, and the relationship between volume and gradation of the deposition with distance from the bank.

DATA

Two digital elevation model surfaces (DEMs) derived from LiDAR datasets were used to analyze floodplain deposition at Elwood Bottoms. The first surface was built from 2012 low water LiDAR with a 1-meter cell spacing. The second LiDAR dataset was collected in January 2021 during low water conditions and was used as the "post-flood" surface. This dataset had 0.6-meter resolution. Both of these datasets were collected by the USACE, Kansas City District.

These DEMs bound the lateral inundation extents of the 2019 flood. Because 95% of the inundated days from 2012 to 2021 (73 of 77) are associated with the large magnitude 2019 event, and this event delivered substantially more sediment per day than the other lower magnitude inundations, this analysis assumes that most of the morphological change can be attributed to the flood. In addition to the LiDAR, ground surveys and sediment samples informed the floodplain analysis. However, for methodological consistency, the authors calculated the change in volume between the two LiDAR datasets.

On March 5, 2021, the authors surveyed and collected sediment samples along five transect lines shown in fig. 3. Transects were surveyed manually with a Trimble R8 Real Time Kinematic (RTK) Global Navigation Satellite System (GNSS) and the Missouri Virtual Reference Station (VRS) Network, which allows GNSS data to be collected and corrected with internet-based RTK positioning at 4 cm horizontal and vertical accuracy.

Sediment samples were collected along the transect lines. A total of 42 samples were collected, 34 of which were collected at the surface and 8 of which were collected approximately 30 cm below the surface. The sample locations were field-selected based on factors such as elevation differences and vegetation differences. Prior to the site visit, the authors only intended to collect surficial samples. However, while in the field, the authors noticed some locations with different gradations at depth. Therefore, subsurface samples were collected at depths of 30 cm below the surface in the case that the deposition from the 2019 flood could not be classified by the surficial

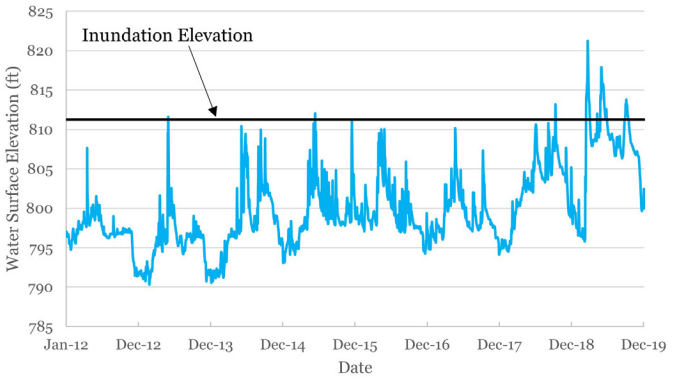

Figure 2. Water surface elevation at St. Joseph USGS gage (06818000), 2012–2019.

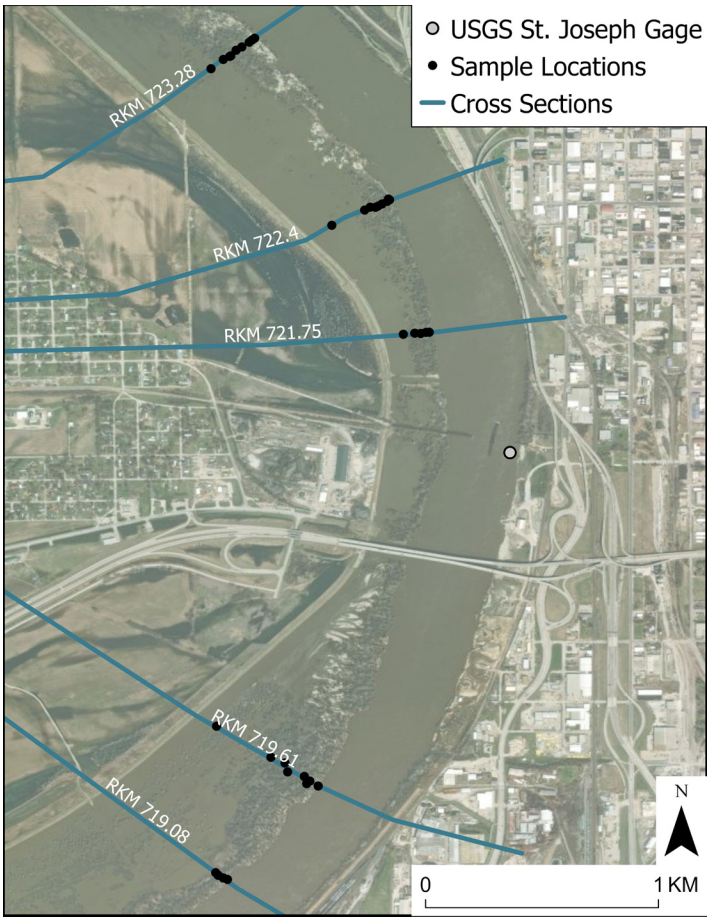

Figure 3. Ground survey and sediment sample locations.

samples alone. If this work were to be replicated, the authors would recommend collecting both surficial and subsurficial samples at each location.

To compare the amount of floodplain deposition to the overall volume change within the river channel, bathymetric surveys were compared before and after the 2019 event. The pre-flood surveys were collected in

2018 (USACE, 2019), and the post-flood surveys were collected in 2021 (USACE, 2022). Each of these datasets were collected with single-beam sonar along cross sections spaced approximately every 500 feet.

METHODS

Floodplain Deposition

The 2012 LiDAR was clipped to the area of interest as the "pre-flood" DEM using ArcGIS. A second DEM was built using the 2021 LiDAR, following Passalacqua et al.'s (2015) method to ensure orthogonality between the two surfaces. The difference between the two raster layers was calculated to create a deposition map. The Surface Volume tool in ArcGIS Pro v 2.8 computed the net volume change between the surfaces.

As a means to quantify error, the authors selected 20 points at locations with constant elevation (e.g., roads, bridges, etc.) and compared the two LiDAR datasets. A similar methodology was used by Haddadchi et al. (2023). The average uncertainty recorded between the datasets at these 20 points was 0.07 meter, both with the mean of errors and the absolute mean of errors (2012 was subtracted from 2021). In other words, there was a 0.07-meter bias in the survey comparison. To correct, 0.07 meter was subtracted from the deposition map as a means to offset the error in the 2012 dataset.

Channel Erosion Analysis

To compare the floodplain deposition with the overall volume change within the Missouri River channel, the authors compared bathymetric surveys from 2018 and 2021. The volume change from 2018 to 2021 was computed using the Cross Section Viewer software tool (Shelley and Bailey, 2018) with cross sections from RKM 723.30 and 719.05. The Cross Section Viewer calculates the volume change between two surveys by an end area method as described in Shelley and Bailey (2018). The longitudinal cumulative volume change can be seen in fig. 4.

Sediment Samples

Personnel from the USACE Engineering Research and Development Center analyzed the fine sediment samples (less than 0.0625 mm) using the wet mode of a Coulter Counter. A small amount of water was added to the samples before they were thoroughly homogenized and sonicated. Vegetated matter was removed from the samples during homogenization. The coarse-grained sediments (greater than 0.0625 mm) were run using the dry power mode of the Coulter Counter. The samples were dried and

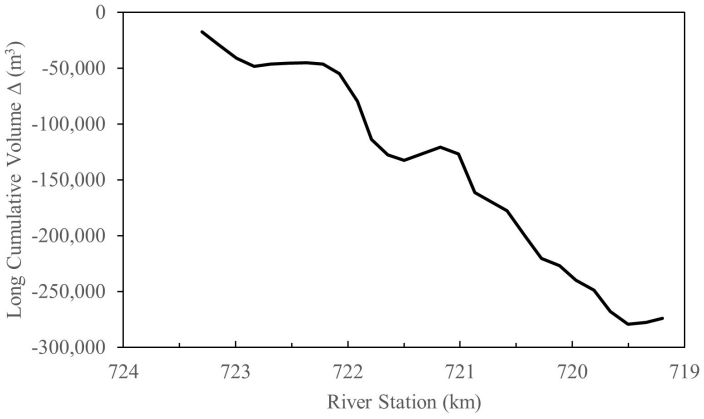

Figure 4. Longitudinal cumulative volume change between RKM 723.30 and RKM 719.05.

disaggregated, if needed (most clumps disaggregated by brushing them through a #10 [2 mm] and #20 [0.85 mm] sieve). All the material passed through a #20 (0.85 mm) sieve and almost all sediment from all samples passed the #35 (0.5 mm) sieve. Organic material retained on the sieves was removed.

Volume of Sand Calculations

Calculating the sand deposition on Elwood Bottoms required interpolating the sand content spatially between the collected sediment samples. The volume of sand was determined by creating two "sand fraction" rasters, one for the top 30 cm and another for the rest of the deposition, corresponding to the two depths at which samples were collected. Measured values of the sand fraction (0 to 1) were extrapolated at each transect along the same trend in the samples (i.e., reflecting how size decreases with distance from the channel) to the edge of the deposition. These spatial sand fraction trends were used to create the sand fraction rasters. To account for vertical variation in the sand fraction, the sand fraction in the subsurface sample was used for any deposition greater than 30 cm, and the sand fraction from the surface sample was used for any deposition less than 30 cm. The following equation was used to compute the sand volume:

$$\text{Sand volume} = (\text{sand fraction}_{0 \text{ to } 30 \text{ cm}} * \text{deposition}_{0 \text{ to } 30 \text{ cm}}) + (\text{sand fraction}_{\text{at } 30 \text{ cm}} * \text{deposition}_{\text{greater than } 30 \text{ cm}})$$

The total sand calculation must account for the decrease in sand with distance from the bank. Computing a total surficial sand volume required spatially weighted averaging to account for the uneven sample spacing. The spatial averaging at four of the five cross sections was performed by linear interpolation between each of the sample locations along the transect. At RKM 722.40, the variation in the sand

fraction was better represented by a power function with respect to the distance from the bank. Due to the limited number of subsurface samples, these extrapolations are more uncertain than the surficial gradations.

RESULTS AND DISCUSSION

Floodplain Deposition Volume and Mapping

Figure 5 presents floodplain elevation difference (i.e., deposition) from 2012 to 2021. Ninety-five percent of the inundation days (73 of 77) from 2012 to 2021 occurred during the 2019 flood. The depth of flood inundation was also much greater during 2019 than the other years, which suggests that nearly all the sediment deposition is attributable to the flood. The area of apparent erosion near the southern end of the study area corresponds with borrow areas used for a levee repair, not flood-related scour. Excluding the borrow areas, the net volume of sediment deposited was 215,000 m^3. Using the spatially averaged sand fraction computed from the sediment samples, the total sand fraction deposited on the floodplain was approximately 93,000 m^3.

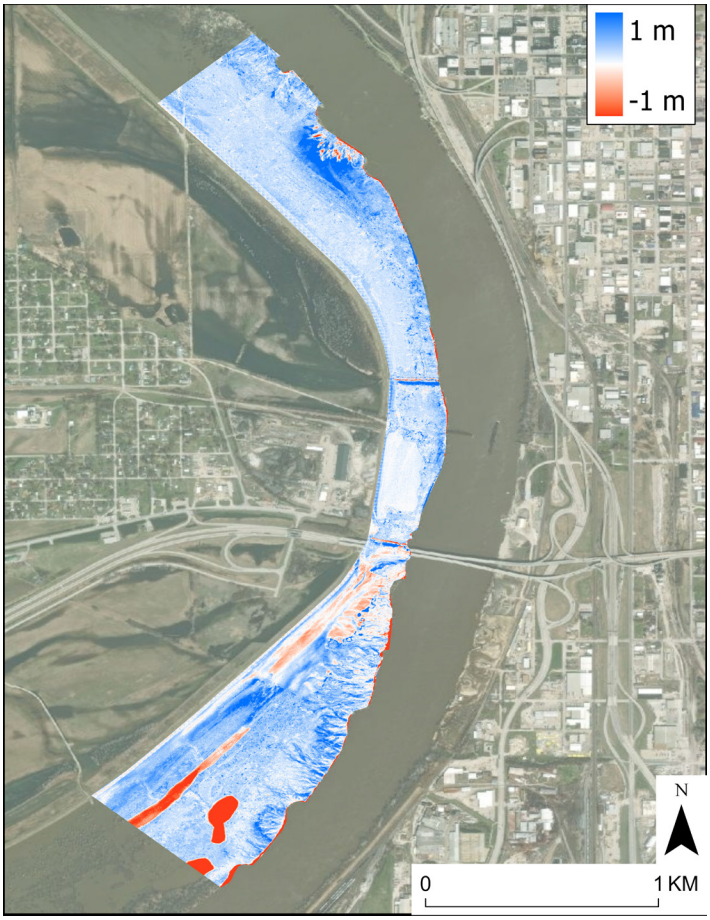

Figure 5. Floodplain deposition on Elwood Bottoms, Kansas, from 2012 to 2021 (blue indicates deposition and red indicates erosion). The dark red near the southern portion of the area of interest is most likely a borrow area used for levee construction and does not represent floodplain erosion.

Floodplain Gradation Trends

Figure 6 presents the results of the sediment size analysis along the five transects. The bottom plot of each pair includes the 2012 LiDAR elevations and the 2021 ground survey transect elevations with the sample sites plotted in their lateral and vertical locations along the survey transect. Green symbols indicate surface sample locations and gray indicate subsurface, so they plot below the survey transect. The upper panes plot the 50th percentile of the grain size distribution (d_{50}) of each of these surficial samples (and subsurface, where applicable). In each case, the sediment fines with distance from the bank. The gradations are plotted on a log scale, so fining in these plots is substantial.

In most cases, the samples collected 200 meters from the channel were at least an order of magnitude finer than the deposits at the banks. The d_{50} values of natural levee deposits next to the river were generally between 0.1 and 0.2 mm (very fine to fine sand). In the distal floodplain (about 200 meters from the channel), the largest grain classes were between 0.01 and 0.02 mm (fine to medium silt). Some of the cross sections fined relatively gradually with distance from the bank, while others reflect more of a step function. The fining trend correlates with floodplain topography: coarser sediment deposited on higher elevation surfaces, and finer sediment deposited in depressions. Transects with abrupt topographic changes (719.08, 721.75, 723.28) have abrupt grain size transitions, and transects with gradual elevation changes (719.61, 722.40) have more gradual size gradation transitions. It is unclear whether topography controls grain size gradation changes or vice versa. As demonstrated in Branß et al. (2016), Lecce and Pavlowsky (2004), and Pizzuto (1987), coarse-grained material is preferentially deposited closer to channel banks, forming natural levees. As the sand load is depleted farther out into floodplain, the depth of deposition decreases and the grain size distribution fines.

Figure 7 includes a more detailed visualization of these distance-gradation floodplain trends, as it plots the distance/elevation-gradation relationship but also includes the grain class components of each sample. The higher elevation samples next to the bank (natural levees) are almost entirely sand, but the sand content drops below 30% for most samples outside this near-channel range as silt and clay dominate more distal samples.

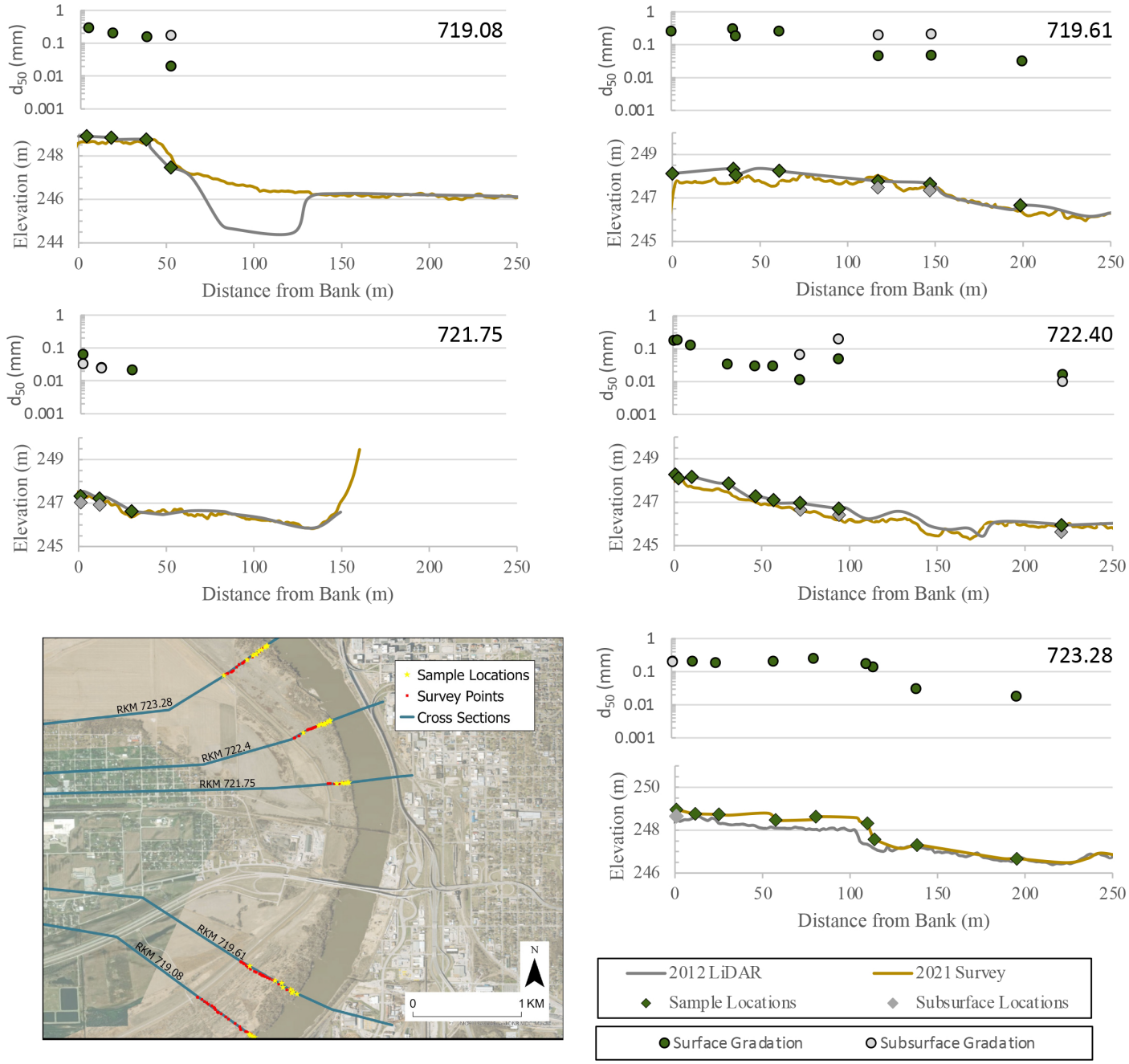

Figure 6. Sediment size vs. distance from the bank. For each of the five transects on the map, the 2012 and 2021 elevations and sample locations are plotted in the bottom pane. The d_{50} values of the samples are plotted in the top pane. (For RKM 721.75, the subsurface and surface d_{50} values at 12 meters from the bank are nearly identical).

The near-bank, higher-elevation, natural levee deposits are composed almost entirely of sand. In most cases, the gradation changes abruptly within approximately 50 meters of the bank. Outside of the near-channel region, the floodplain deposits comprise mostly silt. The clay component increases with distance from the channel as the sand content continues to decrease, driving the d_{90} value down into the silt range.

Figure 8 combines a comparable summary statistic for all the gradation transects on a shared axis, plotting the percent sand with distance from the bank. Solid symbols are surface samples and open symbols are subsurface samples. The percent-sand summary statistic shows trends similar to the d_{90} trends. The surface samples fine with distance from the channel. However, the sand-content data all include abrupt transitions. The floodplain fining

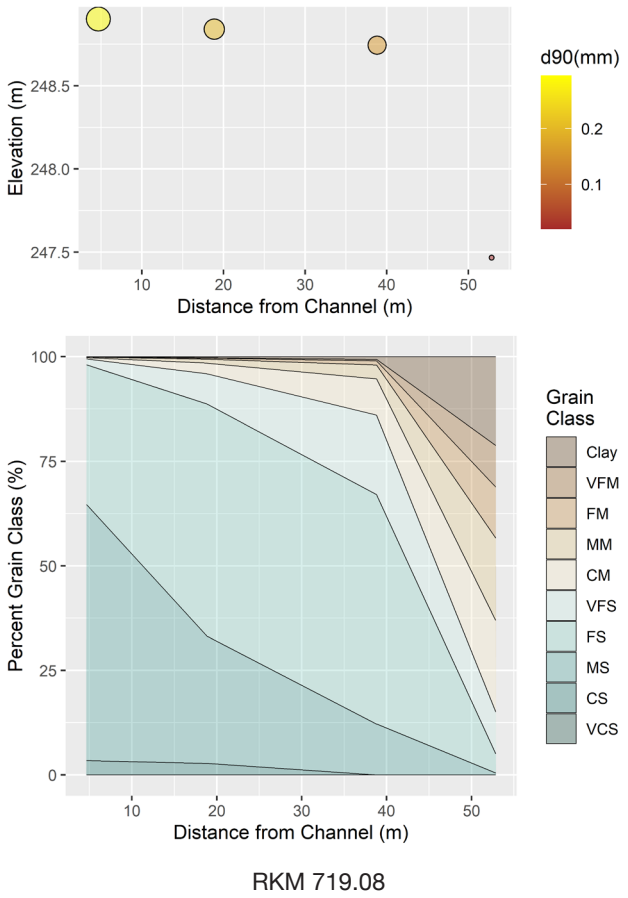

RKM 719.08

RKM 719.61

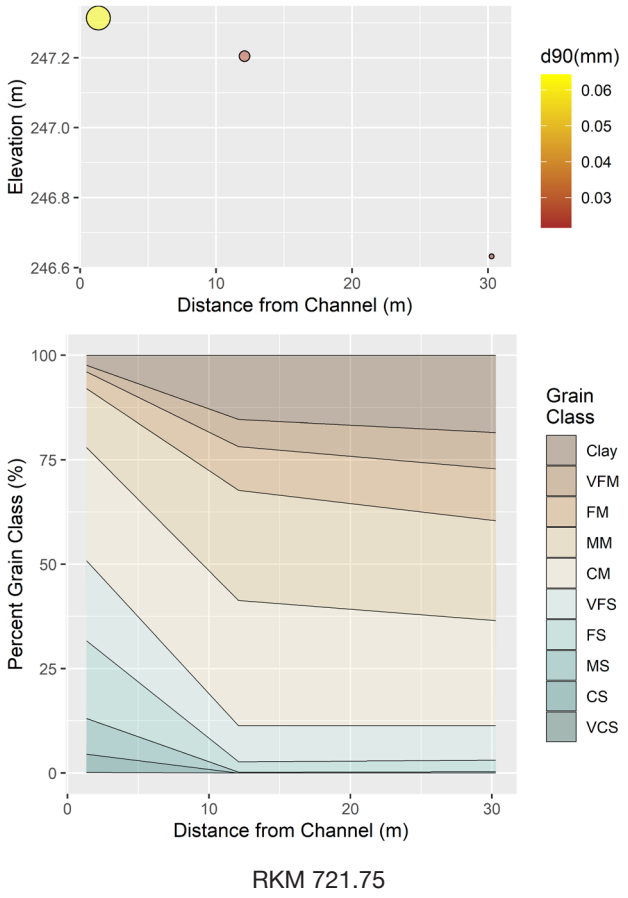

RKM 721.75

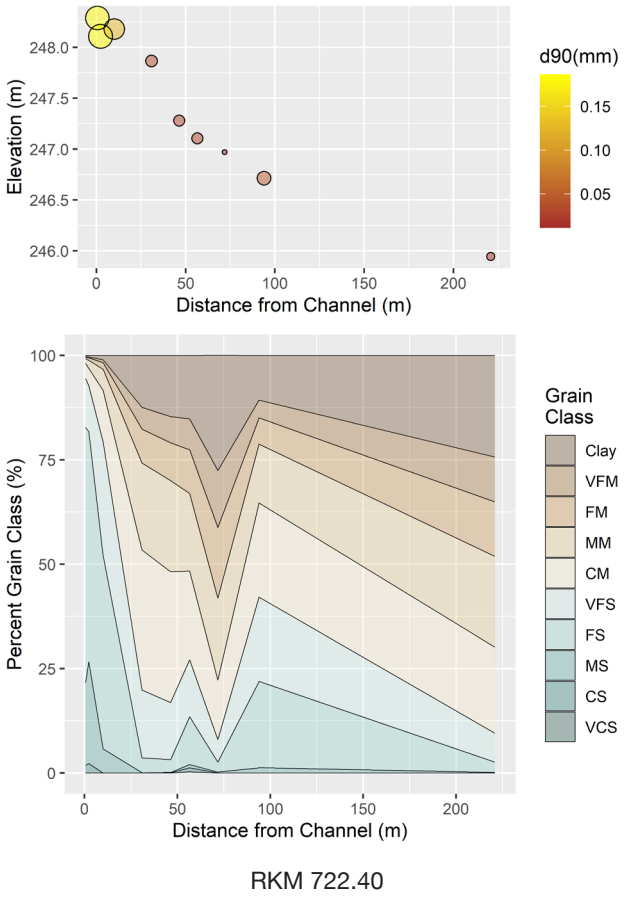

RKM 722.40

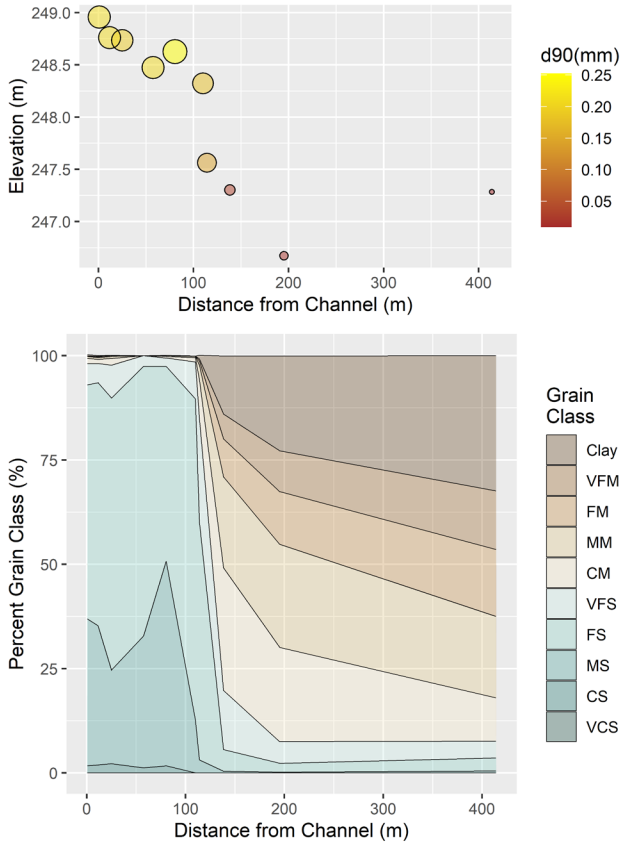

Figure 7. Gradation trend for surficial samples at all five transects. In the top pane for each transect, the size and color of the symbol indicate the size of the d_{90} of the surficial samples collected at the distance from the channel and elevation indicated in the spatial plot. The bottom pane expands the d_{90} summary statistic to illustrate the actual grain class distribution for each of the samples. VFM=very fine silt, FM=fine silt, MM=medium silt, CM=coarse silt, VFS=very fine sand, FS=fine sand, MS=medium sand, CS=coarse sand, VCS=very coarse sand.

trends appear to include two different deposition regimes, a relatively abrupt sand content transition and a gradual silt-and-clay fining trend.

Additionally, the subsurface samples in fig. 8 were coarser than the surface samples at the same locations in seven of the eight samples. In five of the eight samples, the sediment collected 30 cm deep had 30–70% more sand than the surface samples. Transect 721.75 was the counter example to these trends (subsurface samples were similar to or finer than surface samples), but all samples on that transect were collected relatively close to the channel (less than 40 meters from channel bank). The depth-coarsening trend held for samples collected more than 50 meters from the channel. These deposits were most likely from the 2019 event, as the deposition from 2012 and 2021 LiDAR exceeds 30 cm at 56% of the sample locations. Moreover, no vertical layer of organic material was evident in the samples, indicating that sampling at a 30 cm depth had not found the pre-2019 surface.

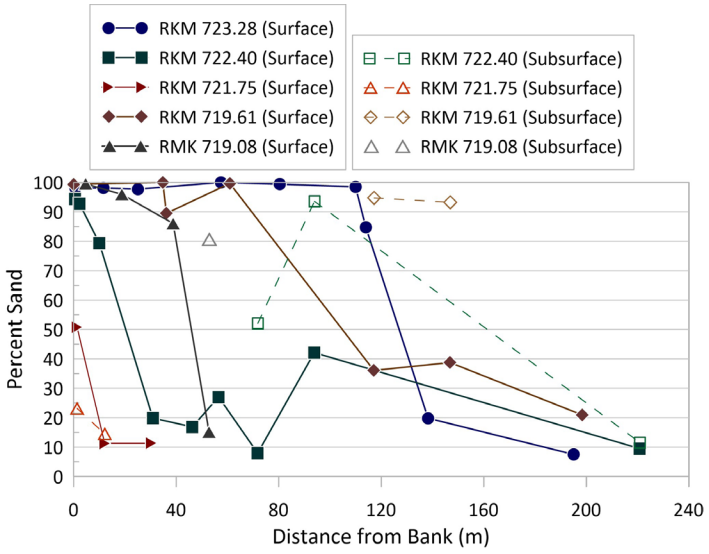

Figure 8. Percent sand vs. distance from the bank.

Relationship Between Floodplain Deposition and Channel Scour

Based upon analysis of bathymetric survey cross sections, the river bed in this reach of the Missouri River (RKM 723.28 to 719.08) degraded 274,000 m^3 from 2018 to 2021. The sand deposition at Elwood Bottoms equates to 35% of that amount, which supports Gibson and Shelley's (2020) finding that floodplain deposition is a significant sediment sink during major Missouri River floods. Gibson and Shelley (2020) hypothesized that floodplain sand deposition, which scaled to total channel erosion, could delay or inhibit channel rebound. The volume of sand deposition computed for the 2019 flood exceeds the value Gibson and Shelley (2020) estimated for the 2011 flood by a factor of 3.5. This could be due to actual differences between the 2011 and 2019 floods; the sediment loads in the extended 2011 event were lower compared to 2019 (USACE, 2017). But the increase could also be due to differences in methodology rather than actual differences in deposition volumes. Gibson and Shelley (2020) associated minimum depth thresholds with remotely sensed polygons that represented a low bound of floodplain deposition. The measurements presented in this study are more precise.

CONCLUSION

The 2019 flood inundated Elwood Bottoms for 73 days and deposited 215,000 m^3 of sediment, including approximately 93,000 m^3 of sand, in and around the Elwood Bottoms floodplain habitat. In most cases, sand was deposited on topographic highs (i.e., the highest elevations) in the 30–50 meters closest to the bank. Sand content dropped to 10–30% by 50 meters from the channel bank in three out of five of the transects, and the deposits continued to fine with distance from the channel as the samples included less sand and more fine silts and clays — material with lower fall velocities. This work is significant in that it confirms previous findings on other large sand-bedded rivers showing that sand deposition on the floodplain is a major sediment sink during flood events. Those developing sediment budgets or sediment models must account for this large sediment sink to accurately characterize geomorphology during floods. Furthermore, this work can be used to calibrate models predicting the morphology and grain size distribution within the floodplain.

ACKNOWLEDGMENTS

Funding for this effort was provided by the U.S. Army Corps of Engineers Regional Sediment Management Program. The authors have no conflicts of interest related to this work. Special thanks to Dereck Wansing for providing survey support and Paul Schroeder for performing the laboratory analyses. The authors would also like to thank Dr. Jim Pizzuto for his review of the first draft of this manuscript, which significantly improved the final version.

DATA AVAILABILITY STATEMENT

Data (LiDAR, ground surveys, and sediment size gradations) that support the findings of this study are available from the corresponding author upon reasonable request.

REFERENCES

Aalto, R., Maurice-Bourgoin, L., Dunne, T., Montgomery, D. R., Nittrouer, C. A., and Guyot, J. L., 2003, Episodic sediment accumulation on Amazonian flood plains influenced by El Niño/Southern Oscillation: Nature, v. 425, no. 6,957, p. 493–497. https://doi.org/10.1038/nature02002

Abraham, D., Ramos-Villanueva, M., Pratt, T., Ganesh, N., May, D., Butler, W., McAlpin, T., Jones, K., Shelley, J., and Pridal, D., 2017, Sediment and hydraulic measurements with computed bed load on the Missouri River, Sioux City to Hermann, 2014: Technical Report, U.S. Army Corps of Engineers, Engineer Research and Development Center, 239 p.

Alexander, J. S., Jacobson, R. B., and Rus, D. L., 2013, Sediment transport and deposition in the lower Missouri River during the 2011 flood: U.S. Geological Survey Professional Paper 1798–F, 27 p. https://doi.org/10.3133/pp1798F

Branß, T., Dittrich, A., and Núñez-González, F., 2016, Reproducing natural levee formation in an experimental flume; *in* G. Constantinescu, M. Garcia, and D. R. Hanes, eds., River Flow 2016: Proceedings of the International Conference on Fluvial Hydraulics: London, Taylor & Francis Group, p. 1,122–1,128.

Gibson, S., and Shelley, J., 2020, Flood disturbance, recovery, and inter-flood incision on a large sand-bed river: Geomorphology, v. 351, 106973. https://doi.org/10.1016/j.geomorph.2019.106973

Haddadchi, A., Bind, J., Hoyle, J., and Hicks, M., 2023, Quantifying the contribution of bank erosion to a suspended sediment budget using boat-mounted LiDAR and high-frequency suspended sediment monitoring: Earth Surface Processes and Landforms, v. 48, no. 14, p. 2,920–2,938. https://doi.org/10.1002/esp.5667

He, Q., and Walling, D. E., 1996, Rates of overbank sedimentation on the floodplains of British lowland rivers documented using fallout ^{137}Cs.: Geografiska

Annaler. Series A, Physical Geography, v. 78, no. 4, p. 223–234. https://doi.org/10.2307/521042

Jacobson, R. B., and Oberg, K. A., 1997, Geomorphic changes of the Mississippi River flood plain at Miller City, Illinois, as a result of the flood of 1993: U.S. Geological Survey Circular 1120-J 22. https://doi.org/10.3133/cir1120J

James, C. S., 1985, Sediment transfer to overbank sections: Journal of Hydraulic Research, v. 23, p. 435–452.

KDWPT, 2022, Elwood Wildlife Area: Kansas Department of Wildlife, Parks, and Tourism. https://ksoutdoors.com/KDWPT-Info/Locations/Wildlife-Areas/Northeast/Elwood

Kiss, T., Oroszi, V. G., Sipos, G., Fiala, K., and Benyhe, B., 2011, Accelerated overbank accumulation after nineteenth century river regulation works: A case study on the Maros River, Hungary: Geomorphology, v. 135, no. 1–2, p. 191–202. https://doi.org/10.1016/j.geomorph.2011.08.017

Lecce, S., and Pavlowsky, R., 2004, Spatial and temporal variations in the grain-size characteristics of historical flood plain deposits, Blue River, Wisconsin, USA: Geomorphology, v. 61, p. 361–371.

Passalacqua, P., Belmont, P., Staley, D. M., Simley, J. D., Arrowsmith, J. R., Bode, C. A., Crosby, C., DeLong, S. B., Glenn, N. F., Kelly, S. A., Lague, D., Sangireddy, H., Schaffrath, K., Tarboton, D. G., Wasklewicz, T., and Wheaton, J. M., 2015, Analyzing high resolution topography for advancing the understanding of mass and energy transfer through landscapes: A review: Earth-Science Reviews, v. 148, p. 174–193. https://doi.org/10.1016/j.earscirev.2015.05.012

Pizzuto, J., 1987, Sediment diffusion during overbank flows: Sedimentology, v. 34, p. 301–307.

Shelley, J., and Bailey, P., 2018, The Cross Section Viewer: A tool for automating geomorphic analysis using cross section data: U.S. Army Engineer Research and Development Center, ERDC/TN RSM-18-3, 9 p. http://dx.doi.org/10.21079/11681/26284

Ten Brinke, W. B. M., Schoor, M. M., Sorber, A. M., and Berendsen, H. J. A., 1998, Overbank sand deposition in relation to transport volumes during large-magnitude floods in the Dutch sand-bed Rhine river system: Earth Surface Processes and Landforms, v. 23, p. 809–824. https://doi.org/10.1002/(SICI)1096-9837(199809)23:9<809::AID-ESP890>3.0.CO;2-1

USACE, 2017, Missouri River bed degradation feasibility study technical report, Appendix C: U.S. Army Corps of Engineers, Kansas City District, 43 p.

USACE, 2019, Updated Missouri River bed changes 2009 to 2018, CENWK-EDH-R memorandum for record, 29 July, 2019: U.S. Army Corps of Engineers, Kansas City District, 18 p.

USACE, 2022, Missouri River bed changes 2009 to 2021, CENWK-EDH-R memorandum for record, 19 January, 2022: U.S. Army Corps of Engineers, Kansas City District, 24 p.

USACE, 2023, Missouri River flow frequency study: Yankton, South Dakota to Hermann, Missouri: U.S. Army Corps of Engineers, 383 p. https://usace.contentdm.oclc.org/utils/getfile/collection/p16021coll7/id/24866

Midcontinent Geoscience • Volume 5 • August 2024
Tony Layzell — Editor

Technical Editor — Julie Tollefson

Suggested citation: Mansfield, M., Shelley, J., and Gibson, S., 2024, Total and sand floodplain deposition on an inside bend during the 2019 Missouri River flood: Midcontinent Geoscience, v. 5, p. 1–10. DOI: https://doi.org/10.17161/mg.v5i.21321

Midcontinent Geoscience is an open-access, peer-reviewed journal of the Kansas Geological Survey. The journal publishes original research on a broad array of geoscience topics, with an emphasis on the midcontinent region of the United States, including the Great Plains and Central Lowland provinces.

Submission information: https://journals.ku.edu/mg/about/submissions

Kansas Geological Survey
1930 Constant Avenue
The University of Kansas
Lawrence, KS 66047-3724
785.864.3965

http://www.kgs.ku.edu/

KANSAS GEOLOGICAL SURVEY
The University of Kansas